

# A System-Theoretic Approach to Bandwidth Estimation

Jörg Liebeherr, *Fellow, IEEE*, Markus Fidler, *Senior Member, IEEE*, and Shahrokh Valaee, *Senior Member, IEEE*

**Abstract**—This paper presents a new foundational approach to reason about available bandwidth estimation as the analysis of a min-plus linear system. The available bandwidth of a link or complete path is expressed in terms of a *service curve*, which is a function that appears in the network calculus to express the service available to a traffic flow. The service curve is estimated based on measurements of a sequence of probing packets or passive measurements of a sample path of arrivals. It is shown that existing bandwidth estimation methods can be derived in the min-plus algebra of the network calculus, thus providing further mathematical justification for these methods. Principal difficulties of estimating available bandwidth from measurements of network probes are related to potential nonlinearities of the underlying network. When networks are viewed as systems that operate either in a linear or in a nonlinear regime, it is argued that probing schemes extract the most information at a point when the network crosses from a linear to a nonlinear regime. Experiments on the Emulab testbed at the University of Utah, Salt Lake City, evaluate the robustness of the system-theoretic interpretation of networks in practice. Multinode experiments evaluate how well the convolution operation of the min-plus algebra provides estimates for the available bandwidth of a path from estimates of individual links.

**Index Terms**—Bandwidth estimation, min-plus algebra, network calculus.

## I. INTRODUCTION

THE benefits of knowing how much network bandwidth is available to an application has motivated the development of techniques that infer bandwidth availability from traffic measurements [6], [11], [15], [17], [20], [28], [32], [34], [39]. With a large number of methods available and much empirical experience gained, recently an increasing effort has been put toward improving the theoretic understanding of measurement-based estimation of available bandwidth, e.g., [5], [26], and [40].

This paper presents a new foundational approach to reason about available bandwidth estimation as the analysis of a min-plus linear system. Min-plus linear system theory has provided the mathematical underpinning for the deterministic network calculus [8], [23]. Drawing from known relationships

between linear system theory and the network calculus, we will use min-plus system theory to explain how bandwidth estimation methods infer information about a network and find bandwidth estimation methods that can extract the most information from a network. Some key difficulties encountered when measuring available bandwidth become evident in a system-theoretic view.

We view bandwidth estimation as the problem of determining unknown functions that describe the available bandwidth based on measurements of a sequence of probing packets or passive measurements of a sample path of arrivals. These functions correspond to the *service curves* that appear in the network calculus, where they are used to express the available service at a network link or an end-to-end path. Working within the context of the network calculus, we can apply a result that allows us to compute the service curve of a network path from service curves of the links of the path. This is done by applying the convolution operator of the min-plus algebra [8], [23]. We explore how well the convolution of the available bandwidth of multiple links, expressed as service curves, can describe the available bandwidth of an end-to-end path.

The contribution of this paper is that it offers an alternative interpretation for bandwidth estimation. Our formulation of available bandwidth in min-plus linear system theory reveals that the underlying estimation problem is intrinsically hard, requiring the solution to a maximin optimization problem. The optimization problem becomes more tractable when the network satisfies the property of “min-plus linearity.” We show that some existing estimation techniques, in particular those in [17] and [34], can be interpreted as analyzing a network with linear input–output relationships. Our derivations reveal properties of existing probing schemes presented in [17] and [34], for example, that these techniques derive the available bandwidth precisely if the network satisfies min-plus linearity. The discovery of an implicit assumption of min-plus linearity in these measurement methods is seemingly at odds with empirical evidence that these methods have been successfully applied in networks that do not satisfy linearity—for example, even a single FIFO link violates the requirements of min-plus linearity. We resolve this apparent contradiction by showing that some networks can be decomposed into disjoint min-plus linear and nonlinear regions. These networks behave as a min-plus linear system at low load and become nonlinear if the load exceeds a certain threshold. The crossing of the linear and nonlinear regions marks the point where the available bandwidth can be observed. A major advantage of formulating the available bandwidth problem in min-plus algebra is that we can exploit the powerful min-plus convolution operator to obtain an estimate of the available bandwidth for end-to-end paths from estimates of constituting links. Additionally, by generalizing the available bandwidth in terms of service curves, we can express multiple

Manuscript received December 31, 2007; revised September 22, 2008 and June 23, 2009; approved by IEEE/ACM TRANSACTIONS ON NETWORKING Editor N. Duffield. First published December 01, 2009; current version published August 18, 2010. This work was supported in part by the National Science Foundation under Grant CNS-0435061, grants from the Natural Sciences and Engineering Council of Canada (NSERC), and an Emmy Noether grant from the German Research Foundation. This is an extended version of a paper that appeared in the Proceedings of IEEE INFOCOM 2007.

J. Liebeherr and S. Valaee are with the Department of Electrical and Computer Engineering, University of Toronto, Toronto, ON M5S 3G4, Canada (e-mail: jorg@comm.utoronto.ca; valaee@comm.utoronto.ca).

M. Fidler is with Leibniz Universität Hannover, Hannover 30167, Germany (e-mail: markus.fidler@ikt.uni-hannover.de).

Digital Object Identifier 10.1109/TNET.2009.2035115

data rates at different time scales. This makes it possible to distinguish a short-term reduction of the data rate due to temporary link congestion from the long-term utilization of a link or a path. This paper also provides an answer to the problem of constructing a best possible passive bandwidth estimation scheme from the measurement of a traffic trace.

The assumptions in this paper on network and traffic characteristics are similar to those in many related works on bandwidth estimation techniques (see Section II). The available bandwidth is represented by a random process, where the source of randomness is the variability of network traffic.

The time scale of network measurements is assumed to be small compared to the time scale at which characteristics of network traffic or network links change. This assumption is a consequence of the requirement for time invariance in min-plus linear system theory. However, it is allowed that the network changes its state between repetitions of a measurement. The assumption of time-invariance is not justified when properties of a network link vary on short time scales, e.g., on wireless transmission channels with random noise. Consequently, such networks are not adequately described in our min-plus system-theoretic formulation.

The remainder of this paper is structured as follows. In Section II, we discuss bandwidth estimation methods and other related work. In Section III, we review the min-plus linear system interpretation of the deterministic network calculus. In Section IV, we formulate bandwidth estimation as the solution to an inversion problem in min-plus algebra. In Section V, we derive solutions to compute the inversion and relate them to probing schemes from the literature. In Section VI, we justify how these probing schemes can be applied in networks that are not min-plus linear. In Section VII, we present measurement experiments of probing schemes suggested by the min-plus system-theoretic concepts from this paper. We present brief conclusions in Section VIII.

## II. AVAILABLE BANDWIDTH ESTIMATION TECHNIQUES

The goal of bandwidth estimation is to infer from measurements a reliable estimate of the unused capacity at a multiaccess link, a single switch, or a network path. The available bandwidth of a network link  $i$  in a time interval  $[t, t + \tau)$  can be specified as [39]

$$\alpha_i(t, t + \tau) = \frac{1}{\tau} \int_t^{t+\tau} [C_i(x) - \lambda_i(x)] dx$$

where  $C_i(t)$  and  $\lambda_i(t)$  are the capacity and total transmitted traffic, respectively, on link  $i$  at time  $t$ . We note that individual definitions of available bandwidth used in the literature may deviate from the above definition. It is generally assumed that link capacities have a constant rate, i.e.,  $C_i(x) = C_i$ . With this, the available bandwidth can be interpreted as a random process, where the randomness stems from the variability of network traffic.

If available bandwidth estimates for single links are available, the available bandwidth of an end-to-end network path with  $H$  links is computed as [18]

$$\alpha(t, t + \tau) = \min_{i=1, \dots, H} \alpha_i(t, t + \tau). \quad (1)$$

Available bandwidth methods measure the transmission of a sequence of control (probe) packets and use the measurements to estimate or bound the available bandwidth. Instead of estimating the available bandwidth, other probing schemes seek to determine the link with the least capacity along a path, given by  $\min_{i=1, \dots, H} C_i$ , and referred to as the *bottleneck capacity*. If the time scale of measurements is small compared to the time scale at which characteristics of network traffic changes, network traffic can be described by a deterministic function. In this case, a single sample of the available bandwidth can be interpreted as being conditioned on the state of the network. Evaluating a large number of samples corresponds to computing a conditional average, which is justified as long as the traffic distribution satisfies stationarity. When network characteristics change on a short time scale, e.g., a wireless channels with random noise, a description of traffic and link by deterministic functions is not suitable.

Almost all proposed probing schemes perform measurements of packet pairs or packet trains. Packet pairs consist of two packets with a defined spacing, and packet trains consist of more than two packets. Since it was first suggested in [16] and [21], packet pair probing has evolved significantly and has been used for estimating the bottleneck capacity (e.g., *Bprobe* [6], *CapProbe* [20]), the available bandwidth (e.g., *ABwE* [31], *Spruce* [39]), and the distribution of cross traffic [27]. The rationale behind these methods builds on the relation of packet dispersion and available bandwidth resources, i.e., packet pairs with a defined gap may be spaced out on slow or loaded links and thus carry information about the network path. Some techniques, e.g., [27] and [39], build on a model of a single link whose capacity is assumed to be known.

The majority of proposed methods employ packet trains for bottleneck capacity estimation (e.g., *PBM* [32], *Cprobe* [6], *pathrate* [11]), and for available bandwidth estimation (e.g., *pathload* [17], *TOPP* [28], *PTR/IGI* [15], and *pathchirp* [34]). The general approach is to adaptively vary the rate of probing traffic to induce congestion in the network. A comprehensive discussion of all techniques is beyond the scope of this paper. For details and empirical evaluations of packet train and packet pair methods, we refer to [18] and [36]–[39]. Some studies have found that packet trains provide more reliable bandwidth estimates than packet pairs [18], [25]. The wide spectrum of bandwidth estimation methods indicates the complexity of measuring available bandwidth in a network. In particular, the comparative evaluations of bandwidth estimation methods sometimes widely disagree in their conclusions on the capabilities and limitations of individual methods.

For the purposes of this paper, the two packet train methods *pathload* and *pathchirp* are particularly relevant. *Pathload* uses a sequence of constant rate packet trains, where the transmission rate of consecutive trains is iteratively varied until it converges to the available bandwidth. In *pathchirp*, the rate is varied within a single packet train using geometrically decreasing interpacket gaps. Both methods interpret increasing delays as an indication of overload, i.e., to detect if the probing rate exceeds the available bandwidth.

Most estimation techniques are designed with an assumption that the network as a whole exhibits the behavior of a single link with constant rate fluid cross traffic. Often it is assumed that the network behaves as a single FIFO system [15], [24]–[29], [34],

[39]. This is justified by the particular packet dispersion of FIFO systems, which is matched by empirical data [29]. It has been found that the best estimates are obtained if the probing traffic increases the load close to, but not beyond, the capacity of the assumed FIFO system.

Some probing methods suggest that probing traffic should follow a Poisson process [25], [32], [39], [44] since it can benefit from the Poisson Arrivals See Time Averages (PASTA) property. Briefly, the PASTA property states that a Poisson arrival process observes the average state of the system. An empirical study [40] found that Poisson probing does not necessarily lead to improved estimates of the available bandwidth. Also, [5] points out that in case of nonintrusive probing, Poisson probing may not be justified since it does not minimize estimation variance when deriving quantities of interest such as available bandwidths.

A set of analytical studies [24]–[26] characterizes the dispersion of probing traffic over single-hop and multihop paths in terms of probing-response curves and extracts the available bandwidth from these curves. Under the assumption of fluid, constant-rate cross traffic, probing-response curves feature a sharp bend at the available bandwidth that is used as criterion by some methods, e.g., TOPP [28]. The mode of operation of many other methods, e.g., the detection of overload by *pathload*, can be related to these curves [25]. Under general bursty cross traffic, the unique turning point of probing-response curves diminishes, whereas it can be recovered under idealized conditions, e.g., using packet trains of infinite length, as shown in [24]–[26].

An alternative approach to sending probe packets is to obtain estimates of the available bandwidth through passive measurements of user traffic. This is the preferred approach in measurement-based admission control (MBAC), which seeks to determine if a network has sufficient resources to support minimal service requirements for a traffic flow or aggregate [7], [19]. In comparison to passive measurements, probing schemes have an additional degree of freedom since they can control the traffic profile of probing packets.

Finally, we discuss prior works that have employed network calculus methodologies in MBAC and bandwidth estimation. Most such works are found in the context of MBAC [7], [19], [41], [43]. Here, it is often assumed, e.g., in [19] and [41], that network nodes provide explicit support for bandwidth measurements. For example, if network nodes support traffic prioritization and transmit probing traffic at the lowest priority, the available bandwidth can be simply expressed as the difference of the node capacity and higher-priority traffic. The authors of [19] and [43] also investigate cross-traffic estimation of wireless channel conditions. End-to-end measurements without network support have been considered in [7]. A major difference to our work is that [7] analyzes bandwidth estimation within a node busy period. In the context of the network calculus, this approach implies the consideration of a specific class of service curves (called *strict service curves* in [23]), which do not naturally extend to a multinode analysis. A broader difference between MBAC and bandwidth estimation is that MBAC operates in the context of providing service guarantees. Here, one generally seeks to obtain a worst-case description of the available service or traffic in terms of time-invariant envelope functions. Worst-case characterizations, even if relaxed to stochastic

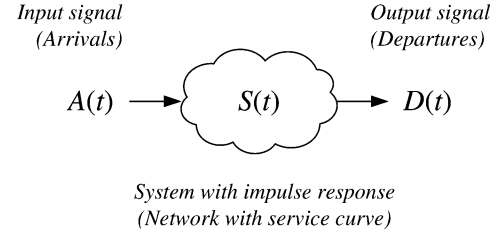


Fig. 1. Linear time-invariant system and min-plus linear network.

bounds, tend to be very conservative. In this paper, we do not use envelopes to describe traffic or service. To our knowledge, the only study that has considered aspects of a min-plus system-theoretic interpretation of available bandwidth is [3]. Under the implicit assumptions of min-plus linearity and convexity of the available bandwidth (concepts that are discussed in detail later in this paper), this study exploits a known relationship between the Legendre transform of a system and its backlog.

### III. MIN-PLUS LINEAR SYSTEM THEORY FOR NETWORKS

This section reviews the linear system representation of networks and introduces needed concepts and notation. We consider a continuous-time setting.

Classical linear system theory deals with linear time-invariant (LTI) systems with input signal  $A(t)$  and output signal  $D(t)$  (see Fig. 1). Linear means that for any two pairs of input and output signals  $(A_1, D_1)$  and  $(A_2, D_2)$ , any linear combination of input signals  $b_1 A_1(t) + b_2 A_2(t)$  results in the linear combination of output signals  $b_1 D_1(t) + b_2 D_2(t)$ . Time-invariant means that for any pair of inputs and outputs  $(A, D)$ , a time-shifted input  $A(t - \tau)$  results in a shifted output  $D(t - \tau)$ .

Let  $S(t)$  be the impulse response of the system, that is, the output signal generated by the system if the input signal is a unity (Dirac) impulse at time zero. The basic property of a LTI system is that it is completely characterized by its impulse response in the sense that the output of the system is expressed as the convolution of the input signal and the impulse response

$$D(t) = \int_{-\infty}^{\infty} A(\tau)S(t - \tau)d\tau =: A * S(t).$$

#### A. Min-Plus Algebra in the Network Calculus

A significant discovery of networking research from the 1990s is that networks can often be viewed as linear systems when the usual algebra is replaced by a so-called min-plus algebra [4], [8], [23]. In a min-plus algebra, addition is replaced by a minimum (we write infimum) and multiplication is replaced by an addition. Similar to LTI systems, a min-plus linear system is a system that is linear under the min-plus algebra. This means that a min-plus linear combination of input functions  $\inf\{b_1 + A_1(t), b_2 + A_2(t)\}$  results in the corresponding linear combination of output signals  $\inf\{b_1 + D_1(t), b_2 + D_2(t)\}$ . In min-plus system theory, the burst function

$$\delta(t) = \begin{cases} \infty, & \text{if } t > 0 \\ 0, & \text{otherwise} \end{cases} \quad (2)$$

takes the place of the Dirac impulse.

Let  $S(t)$  be the impulse response, that is, the output when the input is the burst function  $\delta(t)$ . Any time-invariant min-plus

linear system is completely described by its impulse response, and the output of any min-plus linear system can be expressed as a linear combination of the input and shifted impulse responses by

$$D(t) = \inf_{\tau} \{A(\tau) + S(t - \tau)\} =: A * S(t).$$

In analogy to LTI systems, this operation is referred to as convolution of the min-plus algebra [8].<sup>1</sup> If there exists a function  $S(t)$  such that  $D(t) = A * S(t)$  for all pairs  $(A, D)$ , then it follows that the system is min-plus linear.

The min-plus convolution shares many properties with the usual convolution, e.g., it is commutative and associative. The associativity of min-plus convolution is of particular importance since it implies an easy way of concatenating systems in series. Given a tandem of two min-plus linear systems  $S_1(t)$  and  $S_2(t)$ , the output can be computed iteratively as  $D(t) = (A * S_1) * S_2(t)$  and, with associativity,  $D(t) = A * (S_1 * S_2)(t)$  holds. Generalizing, a tandem of  $N$  systems that are characterized by impulse responses  $S_1, S_2, \dots, S_N$  is equivalent to a single system with impulse response

$$S(t) = S_1 * S_2 * \dots * S_N(t). \quad (3)$$

The observation that some networks can be adequately modeled by a min-plus linear system led to the min-plus formulation of the network calculus [8], [23]. Here, a system is a network element or entire network, input and output functions  $A$  and  $D$  are arrivals and departures, respectively, and the impulse response  $S$ , called the *service curve*, represents the service guarantee by a network element. Network elements that are known to be min-plus linear include work-conserving constant-rate links ( $S(t) = Ct$ , where  $C$  is the link capacity), traffic shapers ( $S(t) = \sigma + \rho t$ , where  $\sigma$  is a burst size and  $\rho$  is a rate), and rate-latency servers ( $S(t) = r(t - d)_+$ , where  $r$  is a rate,  $d$  is a delay, and  $(x)_+ = \max(x, 0)$ ), and their concatenations. As in [8] and [23], we make the convention that functions in the min-plus linear system theory are nondecreasing nonnegative functions that pass through the origin.

The relevance of the network calculus as a tool for the analysis of networks results from an extension of its formal framework to networks that do not satisfy the conditions of min-plus linearity. Nonlinear systems implement more complex mappings  $\Pi$  of arrival to departure functions  $D(t) = \Pi(A)(t)$ . In the network calculus, these are replaced by linear mappings that provide bounds of the form  $D(t) \geq A * \underline{S}(t)$  or  $D(t) \leq A * \overline{S}(t)$  [23, p. xviii]. Here,  $\underline{S}$  is referred to as a *lower service curve* and  $\overline{S}$  is referred to as an *upper service curve*, indicating that they are bounds on the available service. In a min-plus linear system, the service curve  $S$  is both an upper and a lower service curve ( $S = \underline{S} = \overline{S}$ ), which is therefore frequently referred to as *exact service curve*.

### B. Legendre Transform in Min-Plus Linear Systems

In classical linear system theory, the Fourier transform of  $f(t)$ , denoted by  $\mathcal{F}_f(\omega)$ , establishes a dual domain, the frequency domain, for analysis of LTI systems. In the frequency domain, the Fourier transform turns the convolution to a multiplication, that is,  $\mathcal{F}_{f*g}(\omega) = \mathcal{F}_f(\omega) \cdot \mathcal{F}_g(\omega)$ .

<sup>1</sup>We reuse the symbol of the operator for notational simplicity. The context makes this slight abuse of notation nonambiguous.

In min-plus linear systems, the *Legendre transform*, also referred to as convex Fenchel conjugate, plays a similar role. The Legendre transform of a function  $f(t)$  is defined as

$$\mathcal{L}_f(r) = \sup_{\tau} \{r\tau - f(\tau)\}.$$

Since  $r$  can be interpreted as a rate, one may view the domain established by the Legendre transform as a rate domain. The Legendre transform takes the min-plus convolution to an addition [35], that is<sup>2</sup>

$$\mathcal{L}_{f*g} = \mathcal{L}_f + \mathcal{L}_g. \quad (4)$$

Other properties of the Legendre transform that we exploit in this paper are that, for convex functions  $f$ , we have

$$\mathcal{L}(\mathcal{L}_f) = f. \quad (5)$$

In other words, a convex function  $f$  can be recovered from  $\mathcal{L}_f$  by reapplying the Legendre transform [35]. In general, we only have

$$\mathcal{L}(\mathcal{L}_f) \leq f \quad \text{and} \quad \mathcal{L}(\mathcal{L}_f) = \text{conv}_f \quad (6)$$

where  $\text{conv}_f$  denotes the convex hull of  $f$ , defined as the largest convex function smaller than  $f$ .

Another property that will be used is that the Legendre transform reverses the order of an inequality, i.e.,

$$f \geq g \Rightarrow \mathcal{L}_f \leq \mathcal{L}_g. \quad (7)$$

The statement is an equivalency when  $g$  is convex. The potential of the Legendre transform in the network calculus has been previously studied in [3], [12], [14], and [30], generally focusing on the duality of time domain and rate domain. In this paper, we show how the properties of the Legendre transform can be exploited to phrase bandwidth estimation as a new application in the network calculus.

## IV. A MIN-PLUS ALGEBRA FORMULATION OF THE BANDWIDTH ESTIMATION PROBLEM

We view a network as a min-plus linear or nonlinear system that converts input signals (arrivals) into output signals (departures) according to a fixed but unknown service curve  $S$ . The service curve of the network expresses the available bandwidth, which can be a constant-rate or a more complex function. Measurements of a network probe, defined as a sequence of at least two packets, can be characterized by an arrival function  $A^p(t)$  and a departure function  $D^p(t)$ , where the functions represent the cumulative number of bits seen in the interval  $[0, t]$  and time 0 denotes the beginning of the probe. We assume that the system satisfies time-invariance over the duration of a probe. This corresponds to an assumption stated in Section II that network characteristics do not change over the duration of a measurement. The arrival and departure functions of a probe are constructed from timestamps of the transmission and reception of packets and from knowledge of the packet size. In Fig. 2, we illustrate a network probe consisting of five packets of equal size with fixed spacing between the transmission of consecutive packets. The vertical distance between arrivals and departures

<sup>2</sup>Whenever possible, from now on we use the shorthand notation  $f$  to mean “ $f(t)$  for all  $t \geq 0$ ” and  $\mathcal{L}_f$  to mean “ $\mathcal{L}_f(r)$  for all  $r \geq 0$ ”.

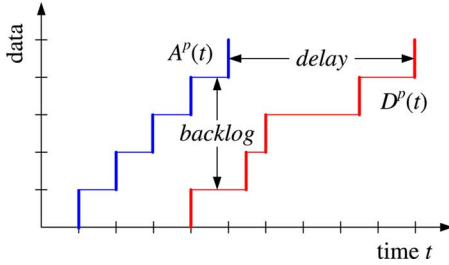


Fig. 2. Example arrival and departure function of a probe of five packets.

is defined as the virtual backlog  $B^p(t) = A^p(t) - D^p(t)$ . The horizontal distance is defined as the delay  $W^p(t)$ .

Representing the network by a min-plus linear system, we interpret a probing scheme as trying to determine from a specific sample of functions  $A^p$  and  $D^p$  an estimate of an unknown lower service  $\underline{S}$ , such that  $D \geq A * \underline{S}$  holds for all pairs  $(A, D)$  of arrival and departure functions. Ideally, the estimate should be a maximal  $\underline{S}(t)$ , i.e., there is no other lower service curve larger than  $\underline{S}(t)$  that satisfies the definition.<sup>3</sup> The goal of a probing scheme is to select a probing pattern, i.e., a function  $A^p$ , that reveals a maximal service curve. A maximal lower service curve  $\underline{S}$  computed from  $A^p$  and  $D^p$  yields a sample of the available bandwidth. Thus,  $\underline{S}$  can be expressed as the solution to the following problem:

$$\begin{aligned} &\text{FIND A MAXIMAL SOLUTION FOR } \underline{S} \\ &\text{SATISFYING } D(t) \geq \inf_{\tau} \{A(\tau) + \underline{S}(t - \tau)\}, \\ &\quad \forall t \geq 0, \text{ for all pairs } (A, D). \end{aligned}$$

Since the service curve is defined in terms of an infimum, determining a maximal service curve has the flavor of a maximin optimization, a class of problems which is fundamentally hard.

The bandwidth estimation problem is easier when the network can be described by a min-plus linear system. As we will see in Section VI, some nonlinear networks, such as FIFO systems, are min-plus linear under low load conditions. Recalling that a system is min-plus linear if it can be described by an exact service curve, the bandwidth estimation problem is reduced to solving the inversion of

$$D(t) = A * S(t) \text{ for all } t \geq 0.$$

Hence, if we take a measurement  $A^p, D^p$  and we can solve  $D^p = A^p * S$  for  $S$ , then, due to min-plus linearity, we have a solution for all possible arrival and departure functions. From Section III, we can infer that a solution is obtained by using the burst function of (2) as probing pattern, i.e.,  $A^p(t) = \delta(t)$ . This follows since the service curve is the impulse response of a min-plus system, that is,  $D^p(t) = \delta * S(t) = S(t)$ . However, sending a probe as a burst function is not practical since it assumes the instantaneous transmission of an infinite-sized packet sequence. While a burst function can be approximated by a sufficiently large back-to-back packet train, a high-volume transmission of probes consumes network resources and interferes with other packet traffic. The observation that large packet trains can lead to unreliable estimates has been noted in the literature [11].

<sup>3</sup>We define a partial ordering of functions such that  $f \leq g$  iff  $f(t) \leq g(t)$  for all  $t$ .

In the next section, we present derivations for three bandwidth estimation methods in min-plus linear systems. We are able to relate two of these methods to previously proposed probing schemes. We will later discuss how these schemes can be applied to certain nonlinear systems.

We conclude this section with remarks on some general aspects of probing schemes and their representations in min-plus linear system theory.

- **Timestamps and asynchrony of clocks:** When clocks at the sender and receiver of a probing packet are perfectly synchronized, and the sender includes the transmission time into each probing packet, the receiver can accurately construct the functions  $A^p$  and  $D^p$ . In practice, however, clocks are not synchronized. When clocks have a fixed offset (but no drift), the arrival function  $A^p$  can be viewed as being time-shifted by an unknown offset  $T$ . In the min-plus algebra a time-shift can be expressed by a convolution, i.e.,  $A^p(t - T) = A^p * \delta_T(t)$  where  $\delta_T(t) = \delta(t - T)$ . Here, the convolution of arrival function and service curve becomes  $(A^p * \delta_T) * \underline{S}$ , which due to associativity and commutativity of the convolution operation, can be rewritten as  $A^p * (\underline{S} * \delta_T)$ . Hence, when the offset is fixed but unknown, even an ideal probing scheme can only compute a service curve that is a time-shifted version of the actual service curve of the network. Drifting clocks make the problem harder. Many bandwidth estimation schemes circumvent the problem of asynchronous clocks by returning probes to the sender [6] or by only recording time differences of incoming probes [15], [17], [28], [34], [39]. A moment's consideration shows that knowledge of the differences between the transmission and arrival of probing packets has the same limitations as dealing with an unknown clock offset  $T$  between the sender and receiver of probing packets.
- **Losses:** Probe packets that are dropped in the network can be thought of as incurring an infinite delay. The presentation of arrival and departure functions in Fig. 2 is not well suited for accommodating packet losses. An alternative presentation, which expresses arrival and departure times of probe packets (on the y-axis) as a function of the sequence numbers (on the x-axis) can deal with packet losses more elegantly, but may appear less intuitive. Such a description of traffic with flipped axes leads to a dual representation of the network calculus that is based on a max-plus algebra [8], [23].
- **Packet pairs:** The arrival and departure functions of a packet pair have each only three points, i.e., the origin and the two timestamps related to the packet pair. If it can be assumed that the service curve has a certain shape, e.g., a rate-latency curve  $S(t) = r \cdot (t - d)_+$ , the service curve can be recovered. In the absence of such an assumption, packet pair methods may not be able to recover more complex service curves. This is reflected in observations that bandwidth estimates from packet pairs tend to be less reliable compared to packet trains if cross traffic is bursty [18], [25].

## V. MIN-PLUS THEORY OF NETWORK PROBING METHODS

In this section, we derive bandwidth estimation methods as solutions to finding an unknown service curve for a min-plus

system. For the derivations, we make a number of idealizing assumptions. First, we consider a fluid flow view of traffic and service. This assumption can be relaxed at the cost of additional notation that accounts for packet sizes of arriving and departing traffic and for the fact that packet transmissions cannot be preempted (see [8] and [23]). Unless stated otherwise, we assume that the network represents a min-plus linear system. This assumption will be relaxed in Section VI. We generally assume that accurate timestamps for transmission and arrival of probes are feasible. If measurements only record time differences between events or include an unknown clock offset between sender and receiver, the computed service curves need to be time-shifted by some constant value.

The derivations of the methods presented in Sections V-B and V-C take advantage of the Legendre transform (see Section III-B). There, we will see that the quality of the estimation depends on convexity properties of the underlying service curve. In fact, these methods can fully recover convex service curves, but only yield the convex hull, i.e., a lower bound, for service curves that are not convex.

#### A. Passive Measurements

We first try to answer the question: *How much information about the available bandwidth can be extracted from passive measurements of traffic?* We first introduce the deconvolution operator of the min-plus algebra, which is defined for two functions  $f$  and  $g$  by

$$f \oslash g(t) = \sup_{\tau} \{f(t + \tau) - g(\tau)\}.$$

The deconvolution operation is *not* an inverse to the convolution ( $f \neq (f \oslash g) * g$ ). However, it has aspects of such an inverse. This is expressed in the following duality statement from [23], which states that for functions  $f, g$ , and  $h$ , the following equivalency holds:<sup>4</sup>

$$f \leq g * h \iff h \geq f \oslash g. \quad (8)$$

We will exploit this property to formulate the following lemma.

*Lemma 1:* For two functions  $g$  and  $h$ , we have

$$((h * g) \oslash g) * g = h * g.$$

*Proof:* The proof makes two applications of (8). Let us define  $\tilde{h} = f \oslash g$  and  $f = g * \tilde{h}$ . By definition of  $\tilde{h}$ , we can conclude with (8) that  $f \leq g * \tilde{h}$ .

By definition of  $f$ , we see from (8) that  $h \geq f \oslash g$ . By our definition of  $\tilde{h}$ , this gives us  $h \geq \tilde{h}$ . From  $h \geq \tilde{h}$  and  $f = g * \tilde{h}$ , we get  $f \geq g * \tilde{h}$ .

Combining the two statements about the relationship of  $f$  and  $g * \tilde{h}$  gives us  $f = g * \tilde{h}$ . Now, by inserting our definition  $\tilde{h} = f \oslash g$ , we obtain  $f = g * (f \oslash g)$ . Inserting our second definition  $f = g * \tilde{h}$  yields  $g * \tilde{h} = g * ((g * \tilde{h}) \oslash g)$ . Reordering the expression using commutativity of the min-plus convolution completes the proof. ■

The lemma justifies the following passive measurement scheme. Let us denote the arrival and departure functions measured from a traffic trace of one or more flows by  $A^p$  and  $D^p$ . By assumption of linearity, we know that  $D^p = A^p * S$

<sup>4</sup>We use shorthand notation  $f = g * h$  to mean “ $f(t) = (g * h)(t)$  for all  $t \geq 0$ .”

holds, but the shape of  $S$  is unknown. Suppose we compute a function  $\tilde{S}$  from the trace as the deconvolution of the departures and the arrivals, i.e., we set

$$\tilde{S} = D^p \oslash A^p. \quad (9)$$

With this, we can derive as follows:

$$\begin{aligned} D^p &= S * A^p \\ &= ((S * A^p) \oslash A^p) * A^p \\ &= (D^p \oslash A^p) * A^p \\ &= \tilde{S} * A^p. \end{aligned}$$

The first equality holds because of our assumption of linearity, the second equality applies Lemma 1, the third uses again the linearity assumption, and the fourth equality follows from inserting (9). We can therefore conclude with Lemma 1 that

$$D^p = A^p * \tilde{S}. \quad (10)$$

Applying the duality property from (8) to  $D^p = A^p * S$ , we obtain  $S \geq D^p \oslash A^p$ . Then, with (9) we have

$$\tilde{S} \leq S.$$

Hence, by deconvolving  $D^p$  and  $A^p$  as in (9), the result  $\tilde{S}$  is a lower service curve, i.e., for all pairs of arrival and departure functions  $(A, D)$ , we have  $D \geq A * \tilde{S}$ . Since, from (10),  $\tilde{S}$  can completely reconstruct the departure function from the arrival function, we can conclude that  $\tilde{S}$  is the best possible estimate of the actual service curve that can be justified from measurements of  $A^p$  and  $D^p$ , in the sense that it extracts the most information from the measurements. Since the above deconvolution computes the largest available bandwidth that can be justified from a given traffic trace, the described method will perform no worse than any existing MBAC method from the MBAC literature [7].

The main drawback of this method is that it can only be applied to linear networks. For networks that do not satisfy min-plus linearity, i.e., that can only be described by a lower service curve ( $D \geq A * \underline{S}$ ) or upper service curve ( $D \leq A * \overline{S}$ ),  $\tilde{S}$  only computes a (not useful) lower bound for an upper service curve  $\overline{S}$ .

*Example: The Dilemma of Passive Measurements:* To illustrate the benefits and limitations of passive measurements for bandwidth estimation, we present an ns-2 simulation [1] of measurements at a single node with capacity  $C$ . There is a propagation delay of 10 ms at the ingress link and a 10-ms delay at the egress link. The packet scheduling algorithm is either FIFO or Deficit Round-Robin (DRR). DRR approximates a fair queuing discipline, which can distribute capacity equally among cross and probe traffic. The cross traffic at this link consists of CBR traffic, which is transmitted in 800-byte packets. The rate of cross traffic is set to half the link capacity. The traffic source for passive measurements is a small segment of 2 s of a high-bandwidth variable bit rate video trace from [10] (the data is from the video trace titled *From Mars to China*). The frame rate is 30 frames per second, the average data rate over the entire segment is 17.1 Mbps, and the peak rate based on the interframe spacing is 154 Mbps. We evaluate the bandwidth estimation, when the link capacity is set to  $C = 70, 50, 30$  Mbps. The resulting service curves are shown in Fig. 3. In each figure, the exact service curve (thick solid line) is a latency rate service

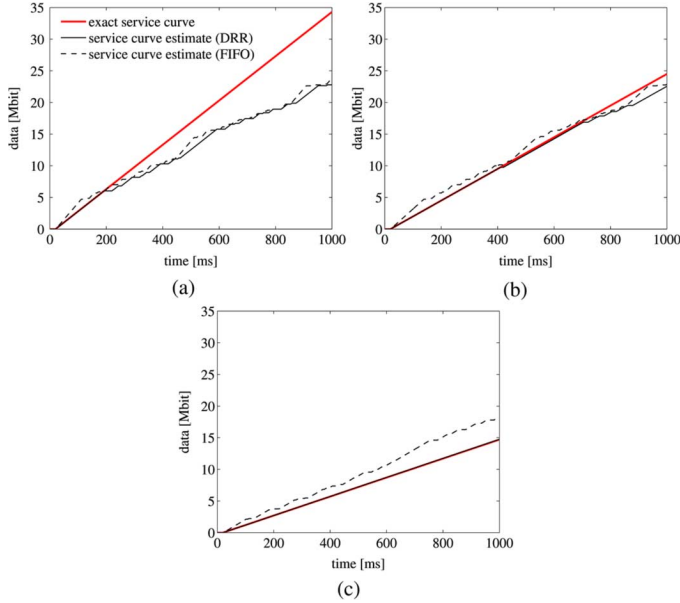


Fig. 3. Example: Passive measurement simulation with a video source. (a)  $C = 70$  Mbps. (b)  $C = 50$  Mbps. (c)  $C = 30$  Mbps.

curve with delay 20 ms and rate  $C/2$ . The computed estimates are indicated by a dashed line for FIFO and a solid line for DRR scheduling. For  $C = 70$  Mbps, the available bandwidth is clearly underestimated. The estimates improve for  $C = 50$  Mbps, where the video trace accounts for a larger fraction of the unused bandwidth. For  $C = 30$  Mbps, the available bandwidth is estimated with high accuracy for the DRR link, but overestimated for the FIFO link. The overly optimistic estimates at a FIFO link occur when the variable bit rate of the video traffic overloads the link, thereby preempting cross traffic. An explanation for this outcome is given in Section VI, where we discuss nonlinearities observed in overloaded FIFO systems. The video trace example indicates a fundamental dilemma with passive measurements. On the one hand, if the traffic intensity of the measured trace is too low, the trace does not extract enough information from the network. On the other hand, if the traffic intensity is too high, the traffic trace may preempt other traffic, thus leading to inaccurate estimates.

### B. Rate Scanning

We now consider an active probing scheme that transmits packet trains at a constant rate, but varies the rate of subsequent trains, e.g., such as *pathload* [17]. We provide a justification for this approach, which we refer to as *rate scanning*, using min-plus system theory.

Given arrival and departure functions  $A$  and  $D$ , using the earlier definition of backlog, the maximum backlog can be computed as

$$B_{\max} = \sup_t \{A(t) - D(t)\}.$$

If the arrivals are a constant rate function, that is,  $A(t) = rt$ , and the network satisfies min-plus linearity, we can write  $B_{\max}$  as a function of  $r$  as follows:

$$\begin{aligned} B_{\max}(r) &= \sup_t \left\{ rt - \inf_{\tau} \{ r\tau + S(t - \tau) \} \right\} \\ &= \sup_t \left\{ \sup_{\tau} \{ r(t - \tau) - S(t - \tau) \} \right\} \\ &= \sup_t \{ rt - S(t) \}. \end{aligned}$$

The first line uses that output in min-plus linear systems can be characterized by  $D = A * S$ . The second line moves the infimum in front of the subtraction, where it becomes a supremum. The third line is a substitution.

Recalling the definition of the Legendre transform from Section III-B, the right-hand side of the last equation can be written as the Legendre transform of  $S$ , that is,  $B_{\max}(r) = \mathcal{L}_S(r)$ . This relation has been observed in [9], [12], and [30]. We now take a further step by applying the relation in the reverse transform. Due to (5), we have for convex service curves  $S$  that

$$S(t) = \mathcal{L}(\mathcal{L}_S)(t) = \mathcal{L}_{B_{\max}}(t) = \sup_r \{ rt - B_{\max}(r) \}.$$

Thus, every convex service curve can be completely recovered by measurements of the maximum backlog  $B_{\max}$ . For service curves that are not convex, we obtain using (6) that

$$\text{conv}_S(t) = \mathcal{L}(\mathcal{L}_S)(t) = \mathcal{L}_{B_{\max}}(t) = \sup_r \{ rt - B_{\max}(r) \}.$$

The convex hull  $\text{conv}_S$  is a lower service curve, that is, a lower bound on the service curve. The quality of the convex hull as a lower bound deteriorates with the distance between the (non-convex) service curve and its convex hull. As long as service elements found in practice are reasonably well described by a latency-rate function (which is convex), their service curves will be close to their respective convex hulls. Even for nonconvex service curves, the convex hull may contain important information. For example, for a leaky-bucket traffic regulator with rate  $r$  and burst size  $b$ , the convex hull recovers the rate parameters  $r$ , but not the burst size  $b$ .

The interpretation of rate scanning is that each constant bit rate stream with rate  $r$  reveals one point  $B_{\max}(r)$  of the service curve in the Legendre domain  $\mathcal{L}_S(r)$ . If we specify a *rate increment*, which sets the rate increase between packet trains and a *rate limit*, which sets the maximum rate at which the network is scanned, we realize a rate scanning method that computes a service curve consisting of piecewise linear segments. The choice of the rate increment determines the length of the segments, and, in this way, the accuracy of the computed service curve. We note that rate scanning is capable of tracking a convex service curve up to a time where the derivative of the service curve reaches the rate limit. The higher the maximum rate, the more information about the service curve is recovered. The number of packets in a packet train must be large enough so that the maximum backlog can be accurately measured.

A criterion for picking the rate limit suggested by our derivations is to stop rate scanning when increasing the scanning rate does not yield an improvement of the service curve. This criterion, however, may fail when the underlying network is not min-plus linear. The rate scanning method *pathload* [17] uses an iterative procedure that varies the rate  $r$  of consecutive packet trains until measured delays indicate an increasing trend. In

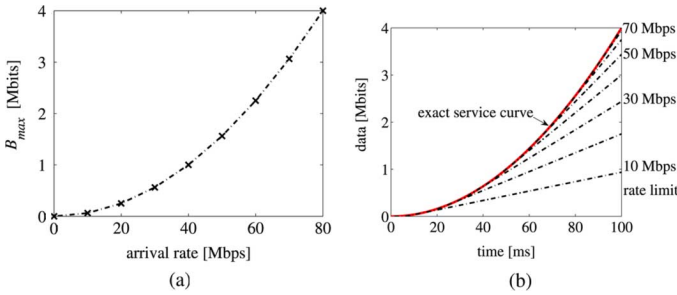


Fig. 4. Service curve estimation with rate scanning. (a) Maximum backlog  $B_{\max}(r)$ . (b) Rate scanning results with different rate limits.

Section VI, we will find that similar criteria can be justified to determine a rate limit in a nonlinear system.

In Fig. 4(a), we present an example of the rate scanning approach for a fluid-flow service curve with a quadratic form  $S(t) = 0.4t^2$ . In the example, rate scanning is performed at rates 10, 20,  $\dots$ , 80 Mbps. In Fig. 4(a), we plot the maximum backlog observed for each scanning rate. The function  $B_{\max}(r)$  is constructed by connecting the measured data points by lines. For rates  $r$  exceeding the rate limit, we can set  $B_{\max}(r) = \infty$  to obtain a conservative Legendre transform for all rate values. This follows from  $\mathcal{L}(\mathcal{L}_S) = \mathcal{L}_{B_{\max}}$  and the order-reversing property of the Legendre transform in (7). In Fig. 4(b), we show the service curves that are obtained with different rate limits. The higher the rate limit, the more accurate the results. Decreasing the increment of the rate will improve the accuracy of the service curve. We point out that both the backlog plot in Fig. 4(a) and the service curves in Fig. 4(b) consist of linear segments.

### C. Rate Chirps

The need of rate scanning to measure a possibly large number of packet trains has motivated the *pathchirp* method [34], where available bandwidth estimates are based on the measurement of a single packet train, with a geometrically decreasing inter-packet spacing. The approach takes inspiration from chirp signals in signal processing, which are signals whose frequencies change with time. We refer to this approach as *rate chirp*, since the decreased gap between packets corresponds to an increase of the transmission rate. We will show that a rate chirp scheme can be justified in min-plus system theory using properties of the Legendre transform.

Suppose we have a lower service curve  $\underline{S}$  satisfying  $D \geq A * \underline{S}$  for all pairs  $(A, D)$ . Taking the Legendre transform we obtain with the order-reversing property of (7) and with (4), that

$$\mathcal{L}_D \leq \mathcal{L}_{A * \underline{S}} = \mathcal{L}_A + \mathcal{L}_{\underline{S}}.$$

We can rewrite this as

$$\mathcal{L}_{\underline{S}} \geq \mathcal{L}_D - \mathcal{L}_A$$

as long as the difference  $\mathcal{L}_D(r) - \mathcal{L}_A(r)$  is defined for all  $r$ . A sufficient condition is that  $\mathcal{L}_A(r) < \infty$  since it prevents both transforms  $\mathcal{L}_D$  and  $\mathcal{L}_A$  from becoming infinite at the same value of  $r$ . Another application of (7) yields

$$\mathcal{L}(\mathcal{L}_{\underline{S}}) \leq \mathcal{L}(\mathcal{L}_D - \mathcal{L}_A).$$

If the system is min-plus linear, that is,  $D = A * S$ , we get

$$\mathcal{L}(\mathcal{L}_S) = \mathcal{L}(\mathcal{L}_D - \mathcal{L}_A).$$

If  $S$  is also convex, then by (5), we have  $S = \mathcal{L}(\mathcal{L}_D - \mathcal{L}_A)$ . As in rate scanning, if  $S$  is not convex, due to (6), applying the Legendre transform twice on the service curve only recovers its convex hull.

This provides us with a justification for *pathchirp* [34] as a probing method. If we depict the transmission of a packet chirp as a fluid flow function, we see that it grows to an infinite rate, thus yielding a Legendre transform that is finite for all rates. By measuring arrivals and departures of the chirp, denoted by  $A^{\text{chrp}}$  and  $D^{\text{chrp}}$ , we can compute a function  $\tilde{S}$  by

$$\tilde{S}(t) = \mathcal{L}(\mathcal{L}_{D^{\text{chrp}}} - \mathcal{L}_{A^{\text{chrp}}})(t). \quad (11)$$

If the network satisfies  $D = A * S$  for all arrivals, then the right-hand side of (11) computes  $\mathcal{L}(\mathcal{L}_S)$ . With (6), we obtain  $\tilde{S} \leq S$ , which tells us that  $\tilde{S}$  is a lower service curve that satisfies  $D \geq A * \tilde{S}$  for any traffic with arrival function  $A$  and departure function  $D$ . If  $S$  is convex, we have  $\tilde{S} = S$ , and we can recover the service curve exactly.

In practical probing schemes, a packet chirp that can grow to an infinite rate is idealized since a rate chirp cannot be transmitted faster than the data rate at the sender of probe packets. For developing a practically useful probing scheme based on rate chirps, we propose modifications that make rate chirp implementable yet comply to the formal requirements of our equations. Suppose a packet chirp is transmitted in a time interval  $[0, t_{\max}^A]$  and  $D$  is observed over an interval  $[0, t_{\max}^D]$ . If we set the value of the arrival function to  $\infty$  past the last measurement at time  $t_{\max}^A$ , we satisfy the requirement that  $\mathcal{L}_A(r) < \infty$ . For the departure function, past the last measurement at  $t_{\max}^D$ , we let the function continue at a rate that corresponds to its slope at time  $t_{\max}^D$ . The following equations express the above extrapolation to the arrival and departure functions:

$$\begin{aligned} \tilde{A}^{\text{chrp}}(t) &= \begin{cases} A^{\text{chrp}}, & \text{if } 0 \leq t \leq t_{\max}^A \\ \infty, & \text{if } t > t_{\max}^A \end{cases} \\ \tilde{D}^{\text{chrp}}(t) &= \begin{cases} D^{\text{chrp}}, & \text{if } 0 \leq t \leq t_{\max}^D \\ D^{\text{chrp}}(t_{\max}^D) + (t - t_{\max}^D) \frac{dD^{\text{chrp}}}{dt}(t_{\max}^D), & \text{if } t > t_{\max}^D. \end{cases} \end{aligned}$$

For convex service curves  $S$ , we can argue that a service curve construction with the above extrapolation yields a lower bound on  $S$ . Let us denote the departures that correspond to an arrival function  $\tilde{A}^{\text{chrp}}$  by  $D^*$ . We will show that  $\tilde{D}^{\text{chrp}} \leq D^*$ , that is,  $\tilde{D}^{\text{chrp}}$  is a lower bound on the departures that correspond to arrivals  $\tilde{A}^{\text{chrp}}$ . To see this, we first observe that, in a min-plus linear system, the function  $D^*$  must be convex. This follows from the convexity of  $\tilde{A}^{\text{chrp}}$ , the relationship  $D = A * S$  that holds for any pair of arrival and departures  $(A, D)$ , and from the fact that the min-plus convolution of two convex functions is again a convex function [23, Th. 3.1.6, p. 136]. By construction,  $\tilde{D}^{\text{chrp}}$  defines the smallest convex extrapolation of  $D^{\text{chrp}}$  for times  $t > t_{\max}^D$  and, consequently,  $\tilde{D}^{\text{chrp}} \leq D^*$ .

Now, evaluating (11) once with  $\tilde{D}^{\text{chrp}}$  and once with  $D^*$ , the order-inverting property of the Legendre transforms yields that a service curve estimate computed from (11) using  $(\tilde{A}^{\text{chrp}}, \tilde{D}^{\text{chrp}})$  is a (conservative) lower bound for the exact service curve of the system.

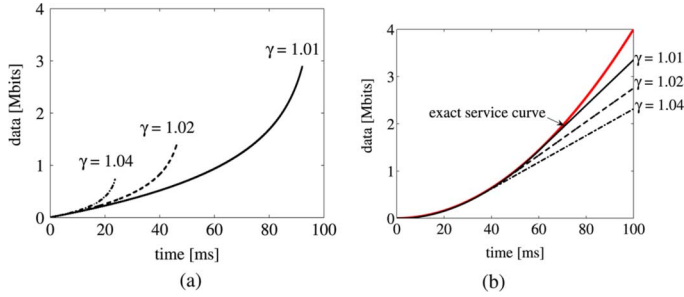


Fig. 5. Service curve estimation with rate chirps. (a) Rate chirps. (b) Rate chirp results with different spread factors.

In Fig. 5(a), we show several rate chirps for a network probe. The rate chirp consists of a step-function that emulates a sequence of probing packets of 1200 bytes. The packets are transmitted at an increasing rate, starting at 10 Mbps and growing to 200 Mbps. The rate is increased by reducing the elapsed time between the transmission of the first bit of two consecutive packets by a constant factor  $\gamma$ , which is called the spread factor in [34]. Larger values for  $\gamma$  lead to shorter chirps that grow faster to the maximum rate. In Fig. 5(b), we show the service curves computed from the chirps in Fig. 5(a). The actual service curve is  $S(t) = 0.4t^2$ , indicated as a thick solid line in the figure. A chirp with a smaller spread factor  $\gamma$ , which transmits more packets over a longer time interval, leads to better estimates of the service curve.

## VI. BANDWIDTH ESTIMATION IN NONLINEAR SYSTEMS

Extending bandwidth estimation to systems that are not min-plus linear, i.e., cannot be described by an exact service curve, raises difficult questions. First, the problem formulation of bandwidth estimation at the beginning of Section IV has shown that the problem has the structure of a maximin optimization. Moreover, in networks with nonlinearities the network service available to a traffic flow may depend on the traffic transmitted by this flow. If this is the case, knowledge of the available bandwidth may not help with predicting network behavior.

In this section, we provide solutions for a class of networks that can be decomposed into disjoint min-plus linear and nonlinear regions. These networks behave like a min-plus linear system at low load and become nonlinear when the traffic rate is increased beyond a threshold. In such a network, the goal of bandwidth estimation should be to determine the available bandwidth of the linear region. The interpretation is that the available bandwidth denotes the maximum additional load that the network can carry without degrading to a nonlinear system. Our work is motivated by studying the available bandwidth at a FIFO link. While we conjecture that most networks can be adequately described by a system that behaves linearly at low loads, the actual scope of this class of networks remains an open problem.

### A. Nonlinearity of FIFO Systems

Consider the FIFO system shown in Fig. 6 with capacity  $C$ . Assume that we have constant-bit rate traffic that is transmitted in 800-byte packets. The FIFO queue experiences (cross) traffic at a rate of  $r_c$ , and probing traffic is sent according to  $A(t) = rt$ . Assuming a link capacity of  $C = 50$  Mbps and cross traffic of  $r_c = 25$  Mbps, we consider a probing rate of

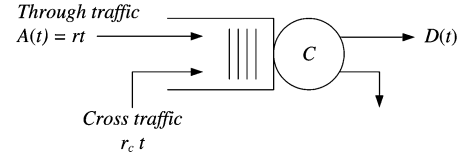


Fig. 6. FIFO system with probe and cross traffic.

TABLE I  
ARRIVAL RATE AND THROUGHPUT OF PROBES IN FIFO

Probe traffic (Mbps)				
Arrival rate	25	50	75	100
Throughput	25	33.3	37.5	40

$r = 25, 50, 75, 100$  Mbps. For an  $ns-2$  simulation of this system, Table I depicts the throughput of the probe packets for different probing rates. As seen previously for passive measurements at a FIFO queue (see Fig. 3), once the probing traffic exceeds the unused capacity, it preempts cross traffic and results in an overly optimistic estimate of the available bandwidth. Empirical observations of FIFO systems with CBR cross and probe traffic in [29] suggested the following departure function:<sup>5</sup>

$$D(t) = \begin{cases} rt, & \text{if } r \leq C - r_c \\ \frac{r}{r+r_c} Ct, & \text{if } r > C - r_c. \end{cases} \quad (12)$$

Thus, if the probing rate is above the threshold  $C - r_c$ , the capacity allocated to the probe and cross traffic is proportional to their respective rates. (Table I illustrates this relationship.) As a result, probing traffic gets more bandwidth when its rate is increased. Note that systems where the allocated rate of a flow increases with its arrival rate violate min-plus linearity.

We now offer a min-plus system interpretation of bandwidth estimation for the depicted FIFO scenario. Consider the function  $S_{\text{fifo}}(t) = [C - r_c]_{+t}$ . From the empirical departure characterization  $D$  of a FIFO system from (12), we can verify that the following is satisfied for all  $t \geq 0$ :

$$\begin{aligned} D(t) &= (rt) * S_{\text{fifo}}, \text{ if } r \leq C - r_c \\ D(t) &\geq (rt) * S_{\text{fifo}}, \text{ if } r > C - r_c. \end{aligned} \quad (13)$$

Therefore,  $S_{\text{fifo}}$  is an exact service curve for  $A(t) = rt$  when  $r \leq C - r_c$ , and  $S_{\text{fifo}}$  is a lower service curve when the arrivals exceed the threshold value. In fact,  $S_{\text{fifo}}$  is the largest lower service curve for a FIFO system and a solution to the maximization in Section IV. Any function larger than  $S_{\text{fifo}}$  may not be a lower service curve for rates  $r > C - r_c$ , indicating that a FIFO system is not min-plus linear in this range.

These considerations suggest to view a FIFO network as a system that is min-plus linear at rates  $r \leq C - r_c$  and crosses into a nonlinear region when the rate exceeds the threshold. The crossing of these regions coincides with the point where the available bandwidth  $S_{\text{fifo}}$  can be observed.

Probing schemes that vary the rate of probe traffic can sometimes be interpreted in terms of searching for the crossover from a linear to a nonlinear regime. In particular, the rules in *pathload* and *pathchirp* to stop measurements when increasing delays are

<sup>5</sup>A proof of this property is found in [13]. We note that closely related models are devised for VBR cross traffic in [25]. While the statistical average of the departures can deviate from (12), the general effect of preemption of cross traffic as in (12) is recovered.

observed can be justified in terms of crossing the nonlinear region (at least in a FIFO system) since a probing rate above  $C - r_c$  is the turning point when the buffer of the FIFO system fills up. In the remainder of this section, we address the problem of locating this crossover point using system-theoretic arguments.

*Remark:* Per our discussion, a FIFO system becomes nonlinear whenever the system is overloaded and a backlog is created. Now, if we consider a FIFO system where discrete-sized packets arrive instantaneously, we can take a position that each packet arrival creates a backlog, and, therefore, each packet arrival makes the FIFO system nonlinear. If we devised a system that detected nonlinearities caused by single packet arrivals, we would only find that the available bandwidth is zero whenever a packet is in transmission, and equal to the capacity otherwise. The issue at hand is one of time granularity. Available bandwidth estimation seeks to determine the unused capacity at a time scale larger than that of a single-packet transmission, specifically at the time scale of a packet train. In our system-theoretic interpretation, we need to be able to observe linearity or nonlinearity at the same time scale, i.e., the duration of a packet train. This adds an implicit assumption that the nonlinearity caused by a single packet arrival can be safely ignored. If this is not the case, our proposed solutions may not apply.

## B. Stopping Criteria

We address the problem of determining the threshold probing rate for a system with disjoint linear and nonlinear regions. The threshold probing rate can be interpreted as the maximum rate at which the network can be probed without leaving the linear region. We refer to a condition that determines the maximum probing rate as a *stopping criterion*.

*Nonlinearity Criterion:* In a min-plus linear system, the service curve is independent of the traffic intensity of the probe traffic. If we have obtained, under assumption of min-plus linearity, a lower service curve  $\tilde{S}$  from a measurement probe with functions  $(A, D)$ , then  $\tilde{S}$  must be a lower service curve for any other arbitrary measurement probe  $(A', D')$ , that is,  $D'(t) \geq A' * \tilde{S}(t)$  for all times  $t$ . A violation of the inequality indicates that the assumption of linearity used for the computation of  $\tilde{S}$  is false.

A simple nonlinearity test can be devised for systems where increased traffic does not result in decreased output. Consider a sequence of probes  $(A_i, D_i)_{i=1,2,\dots,n}$ , where the traffic intensity of subsequent probes is increased, that is,  $A_{i+1} \geq A_i$ . By assumption, we also have  $D_{i+1} \geq D_i$ . Each probe results in an estimate  $\tilde{S}_k(t)$ . If there is a  $k$  for which  $\tilde{S}_k$  violates linearity for some  $i \leq k$ , that is,  $D_i(t) < A_i * \tilde{S}_k(t)$  for some  $t$ , then the network is no longer in the linear region for the probe  $(A_k, D_k)$ .

The described criterion can be directly applied to a rate scanning approach with increasing probing rates where  $A_i(t) = r_i t$  with  $r_{i+1} > r_i$ . As an alternative, one could modify the scanning rate to perform a search for the maximum scanning rate in the linear region. This makes the criterion more similar to the scanning pattern in *pathload*.

Applying the nonlinearity criterion to a rate chirp approach is less straightforward since there is only a single arrival function  $A^{\text{chrip}}$ . Generating multiple arrival functions from a single rate chirp by truncating the arrival functions merely produces truncated versions of the same service curve. Transmitting multiple rate chirps with different spread factors [see Fig. 5(a)] makes

the criterion applicable, yet it loses the main advantage of rate chirps of requiring only a single packet train. Thus, with only a single packet train, we are unable to justify a stopping criterion from min-plus linear systems theory.

*Backlog Convexity Criterion:* This method is applicable to the rate scanning methods, with probing rates  $r \in [r_1, r_2, \dots, r_n]$  with  $r_{i+1} > r_i$ . Assume that the maximum backlog measurement is  $B_{\max}(r)$  for rate  $r$ . Recall from Section V-B that a linear system satisfies  $S(t) = \mathcal{L}_{B_{\max}}(t)$  and  $B_{\max}(r) = \mathcal{L}_S(r)$  holds for all  $r$ . This motivates a test for linearity that exploits properties of the Legendre transform discussed in Section III-B. Under the assumption of linearity, an estimate of the service is obtained from

$$\tilde{S}(t) = \mathcal{L}_{B_{\max}}(t)$$

and  $B_{\max}(r) = \mathcal{L}_{\tilde{S}}(r)$  holds for all  $r$ . Using (5) and (6), if there exists an  $r$  such that  $B_{\max}(r)$  is not convex, i.e.,

$$B_{\max}(r) \neq \text{conv}_{B_{\max}}(r)$$

for some  $r$ , we have  $B_{\max}(r) \neq \mathcal{L}_{\tilde{S}}(r)$ , and hence, the hypothesis of a linear system is dismissed.

For systems that are linear at low probing rates and cross into a nonlinear region after a threshold is reached, a convexity test can be easily devised for schemes that incrementally increase the probing rate. After each rate step, one simply performs a test for equality of  $B_{\max}(r)$  and  $\mathcal{L}(\mathcal{L}_{B_{\max}})(r)$ . If  $B_{\max}(r) \neq \mathcal{L}(\mathcal{L}_{B_{\max}})(r)$ , the system has reached the nonlinear region and the rate scan is terminated. Otherwise, it is assumed that the system is still linear, and the probing rate is increased.

To avoid false positives and negatives in the test for equality, we suggest a heuristic that can account for variability in the measurements. For each value of  $r$ , we compute the difference

$$\Delta B(r) = B_{\max}(r) - \mathcal{L}(\mathcal{L}_{B_{\max}})(r).$$

Note that  $\Delta B(r)$  is nonnegative since  $B_{\max}(r) \geq \text{conv}_{B_{\max}}(r)$ . We define a parameter  $\beta = \Delta B(r)/r$  that expresses the normalized difference. When  $\beta$  exceeds a threshold value, we conclude that the system is no longer in the linear region. We eliminate outliers by running a median filter over  $\beta$  before applying the threshold test. The median filter [33] is a noise-reduction technique, which replaces the value at the center of a sliding window over the data by the median of the window. The design parameter  $\beta$  is used to adjust how quickly nonlinearity is detected in noisy data. A large value of  $\beta$  filters noise effectively but may delay the detection of nonlinearity, and vice versa. In all our experiments,  $\beta = 4$  ms proved balanced.

An additional issue is that since packet trains have a certain length, the maximum backlog  $B_{\max}$  may not be attained by a train. In order to apply the backlog convexity criterion to finite-length packet trains, it must be shown that the backlog that is created by fixed-length packet trains also violates convexity once the boundary to the nonlinear region is crossed. As an example, for FIFO systems, we obtain from (12) that the maximum backlog generated by a packet train of  $L$  bits is

$$B_{\max}^L(r) = \begin{cases} 0, & \text{if } r \leq C - r_c \\ L \cdot \left(1 - \frac{C}{r+r_c}\right), & \text{if } r > C - r_c. \end{cases}$$

For all  $r > C - r_c$  the second derivative of  $B_{\max}^L(r)$  is negative, and thus  $B_{\max}^L(r)$  is strictly concave, while it is convex for  $r \leq C - r_c$ . Thus, the backlog convexity criterion can be applied for finite packet trains in this case.

## VII. EXPERIMENTAL VALIDATION

In this section, we present measurement experiments on an IP network that provide an empirical evaluation of the proposed system-theoretic approach to bandwidth estimation. Specifically, we attempt to provide answers to the following questions:

- How well does the described min-plus system theory that assumes an idealized fluid-flow characterization of traffic and service translate in a packet-based environment?
- How robust are the available bandwidth methods to changes of the distribution of the cross traffic?
- How well is a min-plus system-theoretical approach suitable for finding end-to-end estimates over multiple links?

We conduct a series of measurement experiments on the *Emulab* network testbed at the University of Utah, Salt Lake City [42], where experiments are run on a cluster of PCs that are interconnected by a switched Ethernet network. Propagation delays are emulated by PCs that buffer packets in transmission. *Emulab* provides a realistic IP network environment, yet it offers a controlled lab environment where traffic and resource availability can be explicitly configured. The ability to precisely control network resources enables us to evaluate how well available bandwidth estimates match the configured availability of network resources.

In our experiments, we take advantage of the fact that system clocks in the *Emulab* testbed are synchronized up to 1 ms. According to our discussion in Section IV, if synchronized clocks are not available, then the service curves computed in this section should be interpreted as being horizontally displaced by an unknown amount.

We have implemented the probing schemes for rate-scanning (Section V-B) and rate chirps (Section V-C) using the *rude-crude* traffic generator [22]. In addition, in some experiments we include for benchmark comparison the results of measurements using an unmodified version of the *pathload* software.

We first present measurements on a dumbbell topology as shown in Fig. 7, where each node is realized by a PC of the *Emulab* network. The figure indicates the capacity and the latency of each link. Packet sizes are set to 800 bytes for cross traffic and 1472 bytes for probing traffic. The average data rate of the cross traffic is set to 25 Mbps. The probing method seeks to determine the unused capacity of the link in the center of the figure. The measurements do not address losses of probe traffic. In fact, when a probe packet is dropped, the measurement for this packet is ignored.

### A. Experiment 1: Rate Scanning vs. Rate Chirps

We first compare the effectiveness of the Rate Scanning and Rate Chirp methods from Sections V-B and V-C in the dumbbell topology. We assume that CBR cross traffic is sent at a rate of 25 Mbps.

For the rate scanning method, each packet train has 400 packets, transmitted in increments of 4 Mbps, up to at most 60 Mbps. The stopping criterion is the backlog convexity criterion from Section VI-B with a threshold of  $\beta = 4$  ms and a window size of  $W = 3$  for median filtering.

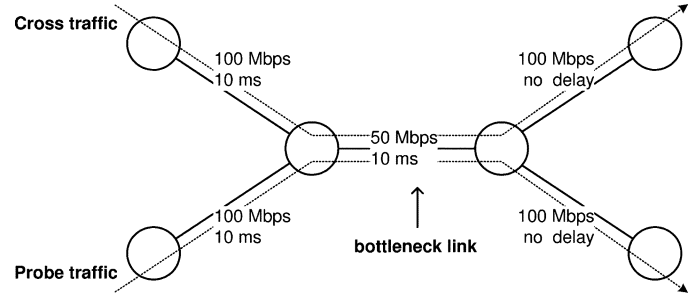


Fig. 7. Dumbbell topology.

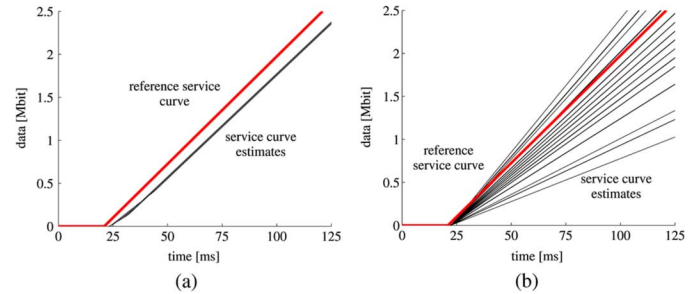


Fig. 8. Experiment 1: Service curve estimates with CBR cross traffic (Each of the graphs shows the reference service curve and the results of 100 repeated estimates of the service curve). (a) Rate Scanning. (b) Rate Chirp.

For the rate chirp method, the initial spacing of probe packets is set to a rate of 4 Mbps, where the spacing between subsequent packets is governed by spread factor of  $\gamma = 1.05$ . The chirp is stopped once its instantaneous rate reaches 100 Mbps, resulting in 66 packets for each chirp. The reason we let the rate chirps go up to 100 Mbps, whereas the rate scans only go up to 60 Mbps, is that data points at the end of the chirps become quite sparse due to the geometric increase of the chirp's rate. For rate chirps, we employ the stopping criterion proposed in [34], which aims at finding the instantaneous data rate at which one-way packet delays start growing due to persistent overload. (Note that an application of the nonlinearity criterion from Section VI-B to the rate chirp method would require multiple rate chirps).

In Fig. 8(a) and (b), we present the results of 100 repeated service curve estimates in terms of the computed service curves for the rate scanning and rate chirp method, respectively. As noted in Section II, each sample of the available bandwidth can be thought of being conditioned on the state of the network. For reference, plotted in a thick solid line, we depict a rate-latency curve with the minimal delay (of approximately 21 ms)<sup>6</sup> and the average available bandwidth (25 Mbps). This curve is referred to as *reference service curve* and serves as an *a priori* bound for the available bandwidth computations.

A comparison of Fig. 8(a) and (b) shows that rate scanning provides more reliable estimates of the service curve than rate chirps. We note that the *pathchirp* method from [34] would yield better results since it smooths the available bandwidth over 11 estimates to deal with the variability of estimates from single rate chirps. Rate scanning and rate chirps perform equally in an ideal linear time-invariant system, while rate chirps are more susceptible to random noise.

<sup>6</sup>The minimal delay consists of 20 ms propagation delay and approximately 1 ms transmission delay.

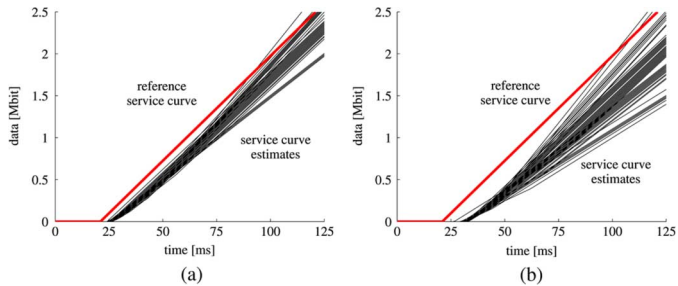


Fig. 9. Experiment 2: Rate scanning with different cross traffic. (a) Exponential cross traffic. (b) Pareto cross traffic.

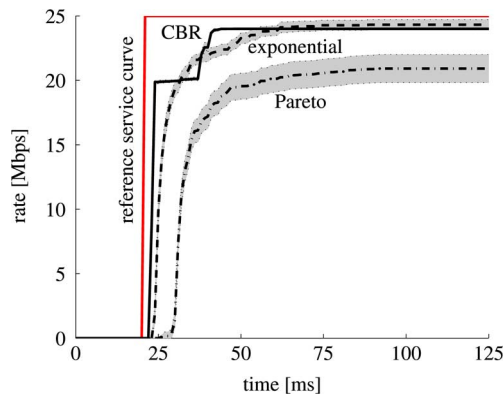


Fig. 10. Results from Experiments 1–2: Derivative of service curves.

In the remaining experiments, we only consider the rate scanning method.

### B. Experiment 2: Different Cross Traffic Distributions.

In this experiment, we evaluate the rate scanning method for different distributions of the cross traffic on the dumbbell topology. We consider cross traffic where interarrivals follow an exponential or Pareto distribution (with shape parameter set to 1.5). All other parameters are as in Experiment 1. In particular, the average traffic rate of cross traffic is 25 Mbps.

In Fig. 9(a) and (b), respectively, we show the results for exponential and Pareto cross traffic. The reference service curve is shown as a thick solid line. It is apparent that, compared to CBR cross traffic in Experiment 1, the higher variance of the cross traffic results in a higher variability of the service curve estimates. At the same time, even for Pareto traffic, almost all estimates of the available bandwidth provide a conservative bound for the reference service curve.

In Fig. 10, we reconcile the results from Figs. 8(a) and 9(a) and (b) in a single graph. We compute the derivatives of the service curves and plot the mean value averaged over the 100 estimates (with 95% confidence intervals). The graph also includes the derivative of the reference service curve (thick solid line). The plot for the reference service curve shows a sudden increase at time 21 ms, where the service curve jumps to a rate of 25 Mbps. The derivatives of the service estimates for CBR, exponential, and Pareto cross traffic provide lower bounds, which become more pessimistic with increasing variance of the cross-traffic distribution.

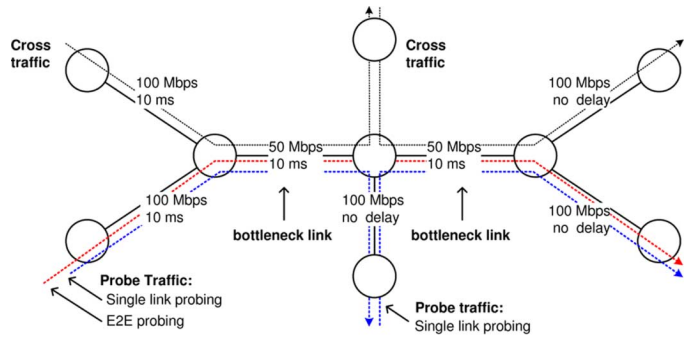


Fig. 11. Topology with multiple bottleneck links.

TABLE II  
PATHLOAD MEASUREMENTS

Cross traffic	lower bound	upper bound
CBR	22.6 Mbps	22.8 Mbps
Exponential	17.7 Mbps	25.4 Mbps
Pareto	15.9 Mbps	29.3 Mbps

As a point of reference, we show in Table II the results of the *pathload* application available from [2] for the same network and cross traffic parameters. *Pathload* is frequently used as a benchmark to evaluate bandwidth estimation techniques. The *pathload* application views available bandwidth as a rate and returns a range that is averaged over a time interval  $\tau$  that bounds the observed distribution of the available bandwidth. For each cross-traffic type, we ran *pathload* 100 times and computed the average values of the lower and upper bounds of the estimated available bandwidth range. A comparison with Fig. 10 shows that the lower bounds of the min-plus theoretic estimation yield service curves, whose long-term average rate is similar to or above the lower bound of *pathload* measurements. As expected, the variation range increases if the cross traffic has a higher variability.

### C. Experiment 3: Multiple Bottleneck Links

We now present measurements over networks with multiple bottleneck links. Fig. 11 depicts the network setup in Emulab with two bottleneck links. The bottleneck links have a capacity of 50 Mbps. The interarrival distribution of cross traffic is exponential with parameters as discussed earlier in this section. As probing scheme, we again use rate scanning with the backlog convexity stopping criterion.

For each network, we compute the end-to-end service curve using two methods. In the first method, called *End-to-End (E2E) Probing*, we send probe traffic end to end over all bottleneck links. In the second method, referred to as *Convolution*, we send probe traffic separately over each bottleneck link and construct a service curve for each link. Then, we compute an end-to-end service curve using the convolution operation following (3). The convolution can be done efficiently in the Legendre domain, where the convolution becomes a simple addition.

Note that in our computation of the available bandwidth over multiple links, the convolution from (3) replaces the minimum in the widely used (1). For the special case that the available bandwidths of links are constant-rate functions, the convolution over multiple links is equal to the minimum of the rates. Formally, if  $S_i(t) = r_i t$  for all  $i$ , we obtain  $S(t) = S_1 * S_2 *$

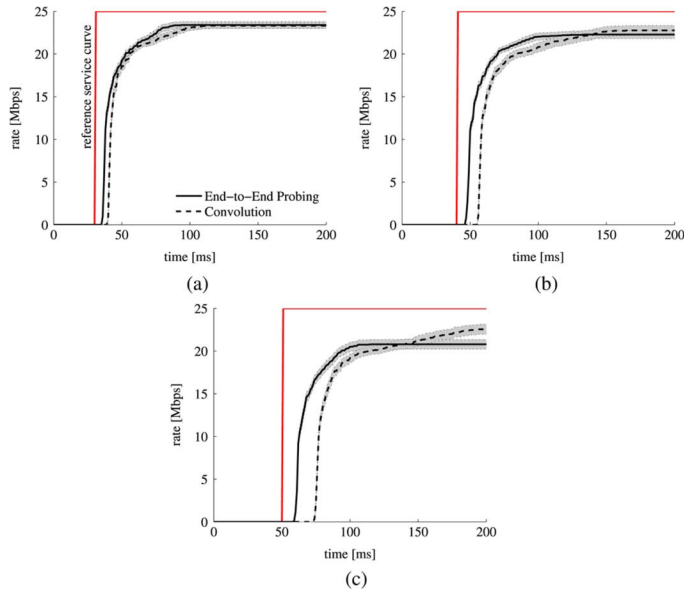


Fig. 12. Experiment 4: Derivative of service curves in multinode measurements. (a) Two bottleneck links. (b) Three bottleneck links. (c) Four bottleneck links.

TABLE III  
PATHLOAD MEASUREMENTS: MULTIPLE BOTTLENECKS

No. bottleneck links	End-to-End probing	Per-link probing with Eq. (1)
2	[14.3, 20.5] Mbps	[15.1, 22.6] Mbps
3	[12.2, 18.2] Mbps	[13.3, 19.9] Mbps
4	[11.7, 17.1] Mbps	[11.8, 18.1] Mbps

$\dots * S_N(t) = \min_i r_i$ . Thus, the convolution expression is a true generalization of the currently prevailing method for composing bandwidth estimation of multiple links.

In Fig. 12(a)–(c), we present the outcomes of our experiments for two, three, and four bottleneck links, respectively. As in Fig. 10, we present derivatives of the service curves. We depict the average values of 100 measurements, as well as the 95% confidence intervals. The reference service curve (thick solid line) is a latency rate service curve with a delay of 10 ms for each traversed bottleneck link and a rate equal to the average unused link capacity. We observe that the results of E2E probing are larger at shorter time scales. Over longer time intervals, the results of the Convolution method yields larger estimates. The long-term average rate of the computed service curves degrades with the number of hops.

In Table III, we show as benchmark the results of *pathload* measurements. We include the range of values of end-to-end probing as well as the results of applying (1) to per-link measurements. The degradation of available bandwidth estimates as the number of bottleneck links is increased is similar as observed in Fig. 12. The long-term average of the service curve in Fig. 12 yields more optimistic results than the range of values in Table III. While the results of the system-theoretic approach for paths with multiple nodes are clearly encouraging, we caution against a generalization to other topologies and production networks.

## VIII. CONCLUSION

We have developed an interpretation of bandwidth estimation as a problem in min-plus linear systems, where the available bandwidth is represented by a service curve. Using service curves as opposed to constant-rate functions permits a description of bandwidth availability at different time scales. We have related difficulties with network probing to nonlinearities of the underlying system. By interpreting a network as a system that is min-plus linear at low loads and becomes nonlinear when the network load exceeds a threshold, we have argued that the crossing of the linear and nonlinear regions marks the point where the available bandwidth can be observed. The success in describing relatively complex probing schemes using min-plus algebra and the ability to concatenate the available bandwidths of multiple links using the min-plus convolution hints at a possibly stronger link between bandwidth estimation and network calculus. In particular, the min-plus convolution operator can be applied to obtain end-to-end estimates from per-link measurements.

## ACKNOWLEDGMENT

The authors thank A. Burchard for many insights and suggestions.

## REFERENCES

- [1] ns-2 network simulator, [Online]. Available: <http://www.isi.edu/nsnam/ns/>
- [2] Pathload, [Online]. Available: <http://www.cc.gatech.edu/fac/Constantinos.Dovrolis/bw-est/pathload.html>
- [3] F. Aghareparast and V. C. M. Leung, "Slope domain modeling and analysis of data communication networks: A network calculus complement," in *Proc. IEEE ICC*, Jun. 2006, pp. 591–596.
- [4] R. Agrawal, R. L. Cruz, C. Okino, and R. Rajan, "Performance bounds for flow control protocols," *IEEE/ACM Trans. Netw.*, vol. 7, no. 3, pp. 310–323, Jun. 1999.
- [5] F. Baccelli, S. Machiraju, D. Veitch, and J. Bolot, "The role of PASTA in network measurement," in *Proc. ACM SIGCOMM*, Pisa, Italy, Sep. 2006, pp. 231–242.
- [6] R. L. Carter and M. E. Crovella, "Measuring bottleneck link speed in packet switched networks," *Perform. Eval.*, vol. 27 and 28, pp. 297–318, 1996.
- [7] C. Cetinkaya, V. Kanodia, and E. W. Knightly, "Scalable services via egress admission control," *IEEE Trans. Multimedia*, vol. 3, no. 1, pp. 69–81, Mar. 2001.
- [8] C.-S. Chang, *Performance Guarantees in Communication Networks*. London, U.K.: Springer-Verlag, 2000.
- [9] R. Cruz, "A calculus for network delay, parts I and II," *IEEE Trans. Inf. Theory*, vol. 37, no. 1, pp. 114–141, Jan. 1991.
- [10] G. Van der Auwera, P. T. David, and M. Reisslein, "Bit rate-variability of h.264/avc Frext," Arizona State Univ., Tech. Rep., Apr. 2006.
- [11] C. Dovrolis, P. Ramanathan, and D. Moore, "What do packet dispersion techniques measure?," in *Proc. IEEE INFOCOM*, Apr. 2001, pp. 905–914.
- [12] M. Fidler and S. Recker, "Conjugate network calculus: A dual approach applying the legendre transform," *Comput. Netw.*, vol. 50, no. 8, pp. 1026–1039, Jun. 2006.
- [13] Y. Ghiassi-Farrokhfal and J. Liebeherr, "Output characterization of constant-bit-rate traffic in fifo networks," *IEEE Commun. Lett.*, vol. 13, no. 8, pp. 618–620, Aug. 2009.
- [14] T. Hisakado, K. Okumura, V. Vukadinovic, and L. Trajkovic, "Characterization of a simple communication network using legendre transform," in *Proc. ISCAS*, May 2003, pp. 738–741.
- [15] N. Hu and P. Steenkiste, "Evaluation and characterization of available bandwidth probing techniques," *IEEE J. Sel. Areas Commun.*, vol. 21, no. 6, pp. 879–894, Aug. 2003.
- [16] V. Jacobson, "Congestion avoidance and control," in *Proc. ACM SIGCOMM*, Aug. 1988, pp. 314–329.
- [17] M. Jain and C. Dovrolis, "Pathload: A measurement tool for end-to-end available bandwidth," in *Proc. PAM Workshop*, Mar. 2002, pp. 14–25.

- [18] M. Jain and C. Dovrolis, "Ten fallacies and pitfalls on end-to-end available bandwidth estimation," in *Proc. ACM IMC*, 2004, pp. 272–277.
- [19] Y. Jiang, P. J. Emstad, A. Nevin, V. Nicola, and M. Fidler, "Measurement-based admission control for a flow-aware network," in *Proc. 1st EuroNGI Conf. Next Generation Internet Netw. Traffic Eng.*, Apr. 2005, pp. 318–325.
- [20] R. Kapoor, L.-J. Chen, L. Lao, M. Gerla, and M. Y. Sanadidi, "Cap-Probe a simple and accurate capacity estimation technique," in *Proc. ACM SIGCOMM*, Aug./Sep. 2004, pp. 67–78.
- [21] S. Keshav, "A control-theoretic approach to flow control," in *Proc. ACM SIGCOMM*, Sep. 1991, pp. 3–15.
- [22] J. Laine, S. Saaristo, and R. Prior, "Rude/Crude," [Online]. Available: <http://rude.sourceforge.net/>
- [23] J.-Y. Le Boudec and P. Thiran, *Network Calculus a Theory of Deterministic Queuing Systems for the Internet*. Berlin, Germany: Springer-Verlag, 2001.
- [24] X. Liu, K. Ravindran, and D. Loguinov, "What signals do packet-pair dispersions carry?," in *Proc. IEEE INFOCOM*, Mar. 2005, pp. 281–292.
- [25] X. Liu, K. Ravindran, and D. Loguinov, "A queuing-theoretic foundation of available bandwidth estimation: Single-hop analysis," *IEEE/ACM Trans. Netw.*, vol. 15, no. 4, pp. 918–931, Aug. 2007.
- [26] X. Liu, K. Ravindran, and D. Loguinov, "A stochastic foundation of available bandwidth estimation: Multi-hop analysis," *IEEE/ACM Trans. Netw.*, vol. 16, no. 1, pp. 130–143, Feb. 2008.
- [27] S. Machiraju, D. Veitch, F. Baccelli, and J. Bolot, "Adding definition to active probing," *ACM SIGCOMM Comput. Commun. Rev.*, vol. 37, no. 2, pp. 19–28, Apr. 2007.
- [28] B. Melander, M. Björkman, and P. Gunningberg, "A new end-to-end probing and analysis method for estimating bandwidth bottlenecks," in *Proc. IEEE GLOBECOM*, Nov. 2000, pp. 415–420.
- [29] B. Melander, M. Björkman, and P. Gunningberg, "First-come-first-served packet dispersion and implications for TCP," in *Proc. IEEE GLOBECOM*, Nov. 2002, pp. 2170–2174.
- [30] J. Naudts, "Towards real-time measurement of traffic control parameters," *Comput. Netw.*, vol. 34, no. 1, pp. 157–167, July 2000.
- [31] J. Navratil and R. L. Cottrell, "ABwE: A practical approach to available bandwidth estimation," in *Proc. PAM Workshop*, Apr. 2003, pp. 1–11.
- [32] V. Paxson, "Measurements and analysis of end-to-end Internet dynamics," Ph.D. dissertation, Univ. California, Berkeley, Apr. 1997.
- [33] I. Pitas and A. N. Venetsanopoulos, *Nonlinear Digital Filters: Principles and Applications*. Norwell, MA: Kluwer, 1990.
- [34] V. Ribeiro, R. Riedi, R. Baraniuk, J. Navratil, and L. Cottrell, "PathChirp: Efficient available bandwidth estimation for network paths," presented at the PAM Workshop, Apr. 2003.
- [35] R. T. Rockafellar, *Convex Analysis*. Princeton, NJ: Princeton Univ. Press, 1972.
- [36] A. Shriram and J. Kaur, "Empirical evaluation of techniques for measuring available bandwidth," in *Proc. IEEE INFOCOM*, May 2007, pp. 2162–2170.
- [37] A. Shriram, M. Murray, Y. Hyun, N. Brownlee, A. Broido, M. Fomenkov, and K. C. Claffy, "Comparison of public end-to-end bandwidth estimation tools on high-speed links," in *Proc. PAM Workshop*, Mar. 2005, pp. 306–320.
- [38] J. Sommers, P. Barford, and W. Willinger, "Laboratory-based calibration of available bandwidth estimation tools," *Microprocess. Microsyst.*, vol. 31, no. 4, pp. 222–235, Jun. 2007.
- [39] J. Strauss, D. Katabi, and F. Kaashoek, "A measurement study of available bandwidth estimation tools," in *Proc. ACM IMC*, 2003, pp. 39–44.
- [40] M. M. Bin Tariq, A. Dhamdhere, C. Dovrolis, and M. Ammar, "Poisson versus periodic path probing (or, does PASTA matter?)," in *Proc. 5th Conf. Internet Meas.*, Oct. 2005, pp. 119–124.
- [41] S. Valaee and B. Li, "Distributed call admission control for ad hoc networks," in *Proc. IEEE 56th VTC*, Sep. 2002, pp. 1244–1248.
- [42] B. White *et al.*, "An integrated experimental environment for distributed systems and networks," in *Proc. OSDI*, Dec. 2002, pp. 255–270.
- [43] D. Wu and R. Negi, "Effective capacity: A wireless link model for support of quality of service," *IEEE Trans. Wireless Commun.*, vol. 2, no. 4, pp. 630–643, Jul. 2003.
- [44] Y. Zhang, N. Duffield, V. Paxson, and S. Shenker, "On the constancy of internet path properties," in *Proc. ACM SIGCOMM Internet Meas. Workshop*, Nov. 2001, pp. 197–211.



**Jörg Liebeherr** (S'88–M'92–SM'03–F'08) received the Ph.D. degree in computer science from the Georgia Institute of Technology, Atlanta, in 1991.

He was on the faculty of the Department of Computer Science at the University of Virginia, Charlottesville, from 1992 to 2005. Since Fall 2005, he has been with the University of Toronto, Toronto, ON, Canada, as Professor of electrical and computer engineering and Nortel Chair of Network Architecture and Services.



**Markus Fidler** (M'04–SM'08) received the doctoral degree in computer engineering from RWTH Aachen University, Aachen, Germany, in 2004.

He was a Post-Doctoral Fellow of NTNU Trondheim, Trondheim, Norway, in 2005 and the University of Toronto, Toronto, ON, Canada, in 2006. During 2007 and 2008, he was an Emmy Noether Research Group Leader at Technische Universität Darmstadt, Darmstadt, Germany. Since 2009, he has been a Professor of information technology at Leibniz Universität Hannover, Hannover,

Germany.



**Shahrokh Valaee** (S'88–M'00–SM'02) received the Ph.D. degree in electrical engineering from McGill University, Montreal, QC, Canada, in 1994.

From 1994 to 1995, he was a Research Associate at INRS Telecom, Montreal, QC, Canada. From 1996 to 2001, he was an Assistant Professor of electrical engineering with Tarbiat Modares University, Teheran, Iran. Since September 2001, he has been an Associate Professor of electrical and computer engineering with the University of Toronto, Toronto, ON, Canada, and holds the Nortel Institute Junior Chair of Commu-

nication Networks.